Description of regional mitral annular nonplanarity in healthy human subjects: A novel methodology

Liam P. Ryan, MD,[a] Benjamin M. Jackson, MD,[a] Yoshiharu Enomoto, MD,[a] Landi Parish, MD,[a] Theodore J. Plappert, CVT,[b] Martin G. St. John-Sutton, MBBS, FRCP,[b] Robert C. Gorman, MD,[a] and Joseph H. Gorman III, MD[a]

Objective: Finite-element analysis demonstrates that the nonplanar shape of the mitral annulus diminishes mitral leaflet stress. It has therefore been postulated that repair with annuloplasty rings that maintain the nonplanar shape of the annulus could increase repair durability. Although the global nonplanarity of the mitral annulus has been adequately characterized, design of such a ring requires a quantitative description of regional annular geometry. By using real-time 3-dimensional echocardiography in conjunction with available image processing software, we developed a methodology for describing regional annular geometry and applied it to the characterization of the normal human mitral annulus.

Methods: Five healthy volunteers underwent mitral valve imaging with real-time 3-dimensional echocardiography. Regional annular height was calculated at 36 evenly spaced intervals.

Results: Maximal annular height/commissural width ratio was found to occur at the midpoint of the anterior annulus in all cases. These values averaged 26% ± 3.1%, whereas those for the midposterior annulus averaged 18% ± 3.0%. The average commissural width was 35.2 ± 6.0 mm. Although substantial spatial heterogeneity was observed, regional annular height at a given rotational position was highly conserved among subjects when normalized to commissural width.

Conclusions: These quantitative imaging and analytic techniques demonstrate that the normal human mitral annulus is regionally heterogeneous in its nonplanarity, and they establish a means of describing annular geometry at a regional level. With wider application, these techniques may be used both to characterize pathologic annular geometry and to optimize the design of mitral valve annuloplasty devices.

From the Harrison Department of Surgical Research,[a] and the Department of Medicine, University of Pennsylvania School of Medicine,[b] Philadelphia, Pa.

Supported by National Institutes of Health grants HL63954 (R.C.G.), HL73021, and HL76560 (J.H.G.), by American Heart Association Post-Doctoral Fellowship 0625455U (L.P.R.), and by a grant from the Claude E. Welch Trust, Massachusetts General Hospital (L.P.R.).

Received for publication Nov 30, 2006; revisions received Jan 31, 2007; accepted for publication Feb 23, 2007.

Address for reprints: Joseph H. Gorman III, MD, University of Pennsylvania School of Medicine, 313 Stemmler Hall, 36th and Hamilton Walk, Philadelphia, PA 19104-4283 (E-mail: gormanj@uphs.upenn.edu).

J Thorac Cardiovasc Surg 2007;134:644-8

0022-5223/$32.00

doi:10.1016/j.jtcvs.2007.04.001

The general nonplanar saddle shape of the human mitral valve (MV) annulus was first described by Levine and colleagues[1,2] by means of early 3-dimensional (3D) echocardiography. This finding has been subsequently corroborated in both human subjects and animal models by several other groups with both invasive and noninvasive imaging techniques.[3-10] To facilitate comparison between annuli and to quantify the global nonplanarity of the annulus, we have previously defined the annular height (AH)/commissural width (CW) ratio (AHCWR). We have subsequently found this parameter to be constant for all normal

Abbreviations and Acronyms

3D = 3-dimensional
AH = annular height
AHCWR = annular height/commissural width ratio
CW = commissural width
MV = mitral valve
rt-3DE = real-time 3-dimensional echocardiography

MVs.[11] Finite-element analysis has demonstrated that annular nonplanarity augments mitral leaflet curvature and thereby substantially reduces leaflet stress.[11] It has been postulated that the current practice of placing flat annuloplasty rings during MV repair may flatten leaflets, thus increasing stress and reducing repair longevity.[11] This speculation has led to an initiative to develop annuloplasty rings that more closely approximate the annular saddle shape and its stress-reducing characteristics.[12,13]

Although high-resolution imaging of both normal and pathologic human MVs has been previously accomplished through the use of both 3D magnetic resonance imaging[10] and real-time 3D echocardiography (rt-3DE),[14,15] regional mitral geometry remains uncharacterized. Rational design of a nonplanar annuloplasty ring cannot proceed in the absence of a high-resolution quantitative description of normal mitral annular geometry. Furthermore, it has been shown that distinct pathologies affect global annular geometry differently.[14] To characterize the distinct patterns of regional annular deformation that arise in conjunction with various valvular and subvalvular pathologies, it is first necessary to develop a method for describing regional annular geometry in quantitative terms and to apply it to healthy subjects. To achieve this goal, this study used state-of-the-art rt-3DE combined with commercially available image processing software and a series of mathematic algorithms to describe quantitatively the normal human mitral annulus along its entire circumference.

Materials and Methods

Image Acquisition

The study was reviewed and approved by the University of Pennsylvania School of Medicine institutional review board. Written informed consent was obtained from each subject. Transthoracic echocardiography was performed in 5 human adult patients without clinical or radiographic evidence of MV pathology. The rt-3DE data sets were acquired with a Sonos 7500 platform (Philips Medical Systems, Andover, Mass) equipped with a 2- to 4-MHz X4 handheld matrix transducer. Gated images were acquired across 8 cardiac cycles. The rt-3DE data sets were exported to a dedicated Cardio-View software (Tomtec Imaging Systems, Munich, Germany) workstation for image manipulation and analysis.

Image Analysis

All analysis was performed at end systole, which was defined as the first frame demonstrating closure of the aortic valve. Image analysis was performed in Cardio-View by visual inspection. Cardio-View allows the interactive manipulation—including rotation, translation, surface rendering, and measurement—of fully 3D ultrasonographic data sets. A rotational template consisting of 18 long-axis cross-sectional planes separated by 10° increments was created. This template was then centered at the geometric center of the MV orifice, aligned with the axis of the mitral orifice, and superimposed on the 3D echocardiogram (Figure 1, *A*). The two annular points intersecting each of the 18 long-axis rotational planes were then identified by orthogonal visualization of each plane; the two points were marked interactively in Cardio-View (Figure 1, *B*). The anterior and posterior commissures were identified, and the distance between them (CW) was measured in Cardio-View. This value was used for all subsequent calculations.

Single-pass spatial smoothing was performed for each set of annular data points with Tecplot software (Amtec Engineering, Bellevue, Wash). The degree of smoothing is determined by a relaxation factor between 0.0 and 1.0; a relaxation factor of 0.5 was used consistently for each data set. We tested the final models to ensure that smoothing did not obliterate or alter the main anatomic conclusions of this work.

Each smoothed data set was then exported to a Matlab environment (The Mathworks, Natick, Mass). The center of gravity of the resultant 36-point data set was translated to the origin. The

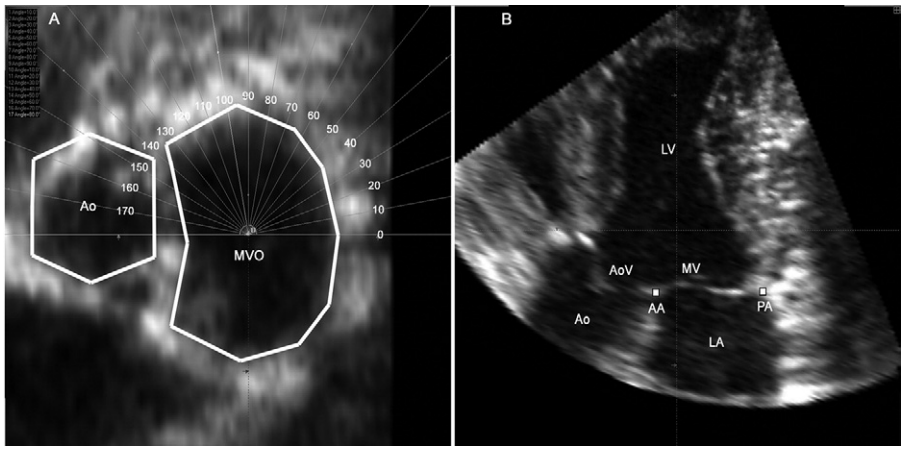

Figure 1. ***A,*** **View of mitral valve in which selected short-axis plane corresponds to plane of mitral valve. Aorta** ***(Ao)*** **and mitral valve orifice** ***(MVO)*** **are indicated. Rotational template consisting of 18 long-axis planes evenly spaced at 10° increments and centered at geometric center of mitral valve has been constructed. B, Single long-axis view (0° on rotational template of panel A) of heart. Left ventricle** ***(LV),*** **mitral valve** ***(MV),*** **left atrium** ***(LA),*** **aortic valve** ***(AoV),*** **and aorta** ***(Ao)*** **are illustrated. Anterior** ***(AA)*** **and posterior** ***(PA)*** **annular points are labeled.**

TABLE 1. Annular geometric parameters for each of 5 subjects

Subject	AH_{Ao} (mm)	AH_{P2} (mm)	CW (mm)	$AH_{Ao}CWR$ (%)	$AH_{P2}CWR$ (%)
1	9.4	7.4	36.2	25.8%	20.3%
2	7.3	4.3	30.4	24.1%	17.9%
3	9.1	5.6	34.6	26.3%	16.1%
4	7.5	4.6	30.2	24.8%	15.2%
5	14.3	10.1	44.8	32.0%	22.6%
Mean ± SD	9.5 ± 2.8	6.4 ± 2.4	35.2 ± 6.0	26.6% ± 3.1%	18.4% ± 3.0%

AH_{Ao}, Annular height adjacent to aorta and midway between commissures; *AH_{P2},* annular height at midpoint of posterior annulus; *CW,* commissural width; *$AH_{Ao}CWR$,* annular height/commissural width ratio adjacent to aorta and midway between commissures; *$AH_{P2}CWR$,* annular height/commissural width ratio at midpoint of posterior annulus.

least squares plane of the 3D data set was then calculated by means of orthogonal distance regression, and the annular model was rotated such that this MV orifice plane was aligned with the xy plane. The z coordinate of each annular point (z_n) was therefore equal to its distance to the plane of the MV. Regional AH for each data point (AH_n) within the annular data set was then defined as $z_n - z_{min}$, where z_{min} was the lowest point on the mitral annulus. Maximal AH (AH_{max}) for a given data set was defined as $z_{max} - z_{min}$, where z_{max} was the highest point on the mitral annulus. As previously described,[11] we use the AH_{max}/CW ratio ($AH_{max}CWR$) to quantify global annular nonplanarity ($AH_{max}/CW \times 100\%$). To facilitate the comparison of regional annular nonplanarity between subjects with different heart sizes, we normalized each value of AH_n for a given subject by the calculated CW of that subject ($AH_n/CW \times 100\%$). We defined this size-normalized index as the regional AHCWR (AH_nCWR). The AH adjacent to the aorta and midway between commissures (AH_{Ao}) was defined as $z_{Ao} - z_{min}$. $AH_{Ao}CWR$ was subsequently defined as $AH_{Ao}/CW \times 100\%$. The AH at the midpoint of the posterior annulus (AH_{P2}) was defined as $z_{P2} - z_{min}$. $AH_{P2}CWR$ was subsequently defined as $AH_{P2}/CW \times 100\%$.

The Cartesian coordinates for each point in a given annular model were converted to cylindrical coordinates (r, θ, z), and the data set was translated in the z direction and rotated around the MV axis (θ direction) so that the data point containing z_{min}, (which in all cases corresponded to the posterior commissure) was located at $z = 0$ and $\theta = 0$. Values of θ and AH_n for each point in a given data set were then recalculated in this fixed frame of reference. Regional AHCWR (AH_nCWR) was plotted as a function of rotational position (θ) on the mitral annulus for each data set.

Results

Individual and mean end-systolic mitral annular parameters are summarized in Table 1. The highest point on the annulus (z_{max}) occurred at the data point corresponding to the aortic portion of the midpoint of the anterior mitral annulus in all cases. Therefore values of AH_{Ao} and $AH_{Ao}CWR$, as reported in Table 1, were equal to AH_{max} and $AH_{max}CWR$, respectively, for each of the 5 subjects. The lowest point on the mitral annulus (z_{min}) occurred at the data point corresponding to the posterior commissure in all cases. The relative heights of the anterior and posterior commissures can be readily appreciated in both Figures 2 and 3.

The mean end-systolic AH at the data point immediately adjacent to the aorta (AH_{Ao}) for the 5 subjects was 9.5 ± 2.8

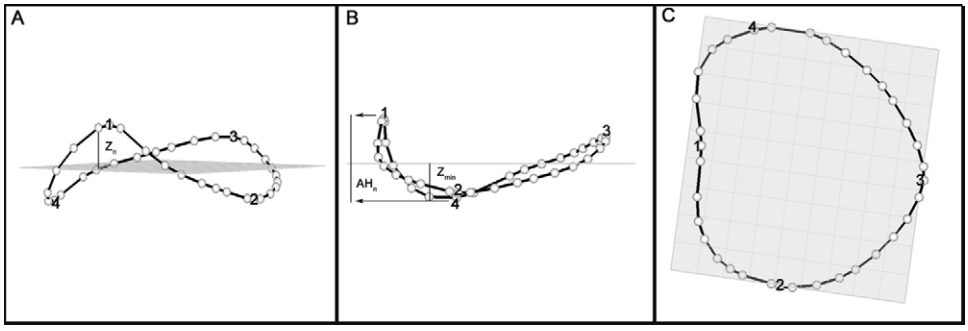

Figure 2. Oblique (A), intercommissural (B), and transatrial (C) views of single human mitral annulus. All 36 data points *(white spheres)* have been included. Aorta *(1),* anterior commissure *(2),* posterior commissure *(4),* and midsegment of posterior annulus *(3)* are labeled in each view. Least square plane is superimposed on annulus in each view. A, How z coordinate for given data point *(z_n)* is measured. B, How regional annular height *(AH_n)* relative to lowest point on mitral annulus *(z_{min})* is calculated. Notice how lowest point coincides with posterior commissure. C, Approximate D shape of annulus.

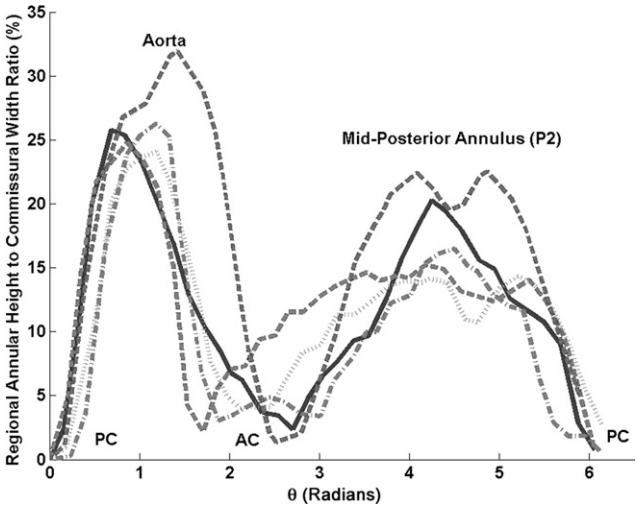

Figure 3. Regional annular height/commissural width ratio is plotted as function of rotational position on mitral annulus *(θ)* for each of 5 subjects on common axis. Posterior commissure *(PC),* aorta, anterior commissure *(AC),* and midposterior annulus *(P2)* are labeled.

mm. The mean end-systolic CW was 35.2 ± 6.0 mm. The mean end systolic AHCWR at the data point adjacent to the aorta ($AH_{Ao}CWR$) was 26.6% ± 3.1%. These measurements are presented in detail for each study subject, along with values of z_{max}, z_{min}, and AH_{P2} (Table 1).

The smoothing algorithm used to minimize pixelation of the annular data and enforce continuity of the anatomic annular model tended to decrease both the AH_{Ao} and the $AH_{Ao}CWR$, but only to a minimal and not statistically significant degree. Expressly, with smoothing, the AH at the aortic point (AH_{Ao}) decreased from 9.8 ± 2.9 to 9.5 ± 2.8 mm ($P = .14$, 1-tailed). Meanwhile, the $AH_{Ao}CWR$ decreased from 27.3 ± 3.4 to 26.6 ± 3.1 mm ($P = .13$, 1-tailed).

Discussion

In this study, we used rt-3DE in conjunction with commercially available image processing software and a series of customized mathematic algorithms to increase our understanding of regional mitral annular geometry in healthy human subjects. Ultimately, these normal regional data can be used to compare patterns of annular deformation in subjects with different valvular or subvalvular pathologies and describe them in quantitative terms. Additionally, establishment of the normal relationship between regional AH and rotational position along the mitral annulus allows these data to be incorporated into the ongoing refinement of MV repair techniques and devices.

Eighteen years ago, Levine and colleagues[1,2] used nascent 3D echocardiographic technology to describe the nonplanar saddle shape of the mitral annulus for the first time. Subsequently, our group used a combination of sonomicrometry and second-generation rotational 3D echocardiography to quantify the maximal nonplanarity of the mitral annulus by describing the AHCWR.[11] With this parameter for quantification, we discovered that the global saddle shape (maximal nonplanarity) of the mitral annulus was conserved across a number of mammalian species, including human beings. In all animals studied, we found the AHCWR to be approximately 20%.[11] In this study, we report substantially larger values. We believe that the discrepancy is likely a result of technical limitations inherent to the rotational technique used in the earlier study, in which the axis of rotation was selected visually during image acquisition and the 18 imaging planes were based on this initial selection. Consequently, relatively large segments of the mitral annulus may not have been imaged. As can be appreciated in Figure 3, AH varies substantially with relatively small rotational increments, particularly adjacent to the commissures and the aortic peak of the midanterior annulus. Because the positions of these landmarks in 3D space determine AH, a relatively small error in assigning their positions results in a significant decrease in both global AH and AHCWR. This would be the case if 1 of the 18 rotational planes determined by the initial axis selection did not pass through or relatively near the commissures or the aortic peak and may explain the apparent underestimation in the earlier study. In this study, the rotational axis was selected off-line, when the entire mitral annulus was visible. It was therefore possible to ensure both uniform marker spacing and inclusion of critical landmarks, such as the commissures and the aortic peak, which determine global AH and AHCWR. We believe that the current methodology allows a more accurate description of global annular nonplanarity.

With numeric simulation and geometric simplification, we have previously demonstrated that alterations in annular saddle shape are capable of affecting both leaflet curvature and stress distribution patterns.[11] By means of this theoretic analysis, we also demonstrated that for any defined load and leaflet geometry, leaflet stress reaches a minimum at ACHWR values between 15% and 30% and increases exponentially as ACHWR approaches zero (as the annulus approaches planarity). It is interesting to note that all AHCWR values reported in this study fall either within or very nearly within this ideal range.

This earlier work, in conjunction with a growing understanding that MV repair durability is not as robust as once thought,[16-20] has spawned a growing interest in the design of nonplanar annuloplasty rings. Nearly all current MV repair techniques include placement of a flat annuloplasty ring. These rings obliterate the annular saddle shape, which flattens the leaflets, thus increasing stress[11] and potentially

limiting repair durability. In this study, we used modern rt-3DE technologies in conjunction with commercially available image processing software and a series of novel, customized mathematic algorithms to increase our understanding of regional mitral annular geometry. These quantitative geometric insights have direct implications for the design of annuloplasty devices that maintain or restore normal annular 3D shape.

After adjustment to account for differing definitions of AH, the global AHCWR values presented in this study are similar to those reported elsewhere through the use of rotational echocardiography and magnetic resonance imaging.[10,14] The analytic techniques that we describe, however, allow the quantification of regional annular geometry with exceptional spatial resolution. This regional assessment demonstrates that regional nonplanarity is heterogeneous in healthy human subjects. Both regional AH and the rate at which this height changes as a function of rotational position are substantially higher across the anterior annulus than the posterior annulus.

Despite the significant regional heterogeneity of AH observed in this study, our data demonstrate that regional AH variations, after normalization by the associated CW, are highly conserved among healthy individuals. Nonplanar annuloplasty rings that conform to native geometry can be thus constructed in a uniform manner with the only independent variable as the predicted native CW. With future studies involving more patients, the relationship between intercommissural dimension and regional height can be also correlated with patient size, thus further facilitating ring selection before elective surgery.

This study establishes the relationship between AH and rotational position in healthy human subjects, as well as quantitative indices with which to describe it. As additional patients with various valvular and subvalvular pathologies are studied, the analytic techniques we describe can also be used to characterize their associated patterns of annular deformation with reference to normal regional geometry. Furthermore, as this technique is applied to large numbers of patients with mitral regurgitation before and after repair, geometric predictors of both surgical and clinical outcomes may begin to emerge. This may ultimately allow surgeons to select a repair strategy preoperatively by quantitative means rather than by relying solely on intraoperative intuition and may thereby contribute to the continued refinement of MV repair techniques and devices.[21]

ACD

References

1. Levine RA, Triulzi MO, Harrigan P, Weyman AE. The relationship of mitral annular shape to the diagnosis of mitral valve prolapse. *Circulation.* 1987;75:756-67.
2. Levine RA, Handschumacher MD, Sanfilippo AJ, Hagege AA, Harrigan P, Marshall JE, et al. Three-dimensional echocardiographic reconstruction of the mitral valve, with implications for the diagnosis of mitral valve prolapse. *Circulation.* 1989;80:589-98.
3. Gorman JH 3rd, Gupta KB, Streicher JT, Gorman RC, Jackson BM, Ratcliffe MB, et al. Dynamic three-dimensional imaging of the mitral valve and left ventricle by rapid sonomicrometry array localization. *J Thorac Cardiovasc Surg.* 1996;112:712-26.
4. Flachskampf FA, Chandra S, Gaddipatti A, Levine RA, Weyman AE, Ameling W, et al. Analysis of shape and motion of the mitral annulus in subjects with and without cardiomyopathy by echocardiographic 3-dimensional reconstruction. *J Am Soc Echocardiogr.* 2000;13:277-87.
5. Kaplan SR, Bashein G, Sheehan FH, Legget ME, Munt B, Li XN, et al. Three-dimensional echocardiographic assessment of annular shape changes in the normal and regurgitant mitral valve. *Am Heart J.* 2000;139:378-87.
6. Timek TA, Green GR, Tibayan FA, Lai DT, Rodriguez F, Liang D, et al. Aorto-mitral annular dynamics. *Ann Thorac Surg.* 2003;76:1944-50.
7. Ahmad RM, Gillinov AM, McCarthy PM, Blackstone EH, Apperson-Hansen C, Qin JX, et al. Annular geometry and motion in human ischemic mitral regurgitation: novel assessment with three-dimensional echocardiography and computer reconstruction. *Ann Thorac Surg.* 2004;78:2063-8.
8. Gorman JH 3rd, Jackson BM, Enomoto Y, Gorman RC. The effect of regional ischemia on mitral valve annular saddle shape. *Ann Thorac Surg.* 2004;77:544-8.
9. Kwan J, Qin JX, Popovic ZB, Agler DA, Thomas JD, Shiota T. Geometric changes of mitral annulus assessed by real-time 3-dimensional echocardiography: becoming enlarged and less nonplanar in the anteroposterior direction during systole in proportion to global left ventricular systolic function. *J Am Soc Echocardiogr.* 2004;17:1179-84.
10. Kaji S, Nasu M, Yamamuro A, Tanabe K, Nagai K, Tani T, et al. Annular geometry in patients with chronic ischemic mitral regurgitation: three-dimensional magnetic resonance imaging study. *Circulation.* 2005;112(9 Suppl):I409-14.
11. Salgo IS, Gorman JH 3rd, Gorman RC, Jackson BM, Bowen FW, Plappert T, et al. Effect of annular shape on leaflet curvature in reducing mitral leaflet stress. *Circulation.* 2003;106:711-7.
12. Tibayan FA, Rodriguez F, Langer F, Zasio MK, Bailey L, Liang D, et al. Annular remodeling in chronic ischemic mitral regurgitation: ring selection implications. *Ann Thorac Surg.* 2003;76:1549–5.
13. Gorman JH 3rd, Gorman RC, Jackson BM, Enomoto Y, St John-Sutton MG, Edmunds LH Jr. Annuloplasty ring selection for chronic ischemic mitral regurgitation: lessons from the ovine model. *Ann Thorac Surg.* 2003;76:1556-63.
14. Watanabe N, Ogasawara Y, Yamaura Y, Wada N, Kawamoto T, Toyota E, et al. Mitral annulus flattens in ischemic mitral regurgitation: geometric differences between inferior and anterior myocardial infarction: a real-time 3-dimensional echocardiographic study. *Circulation.* 2005;112(9 Suppl):I458-62.
15. Watanabe N, Ogasawara Y, Yamaura Y, Kawamoto T, Toyota E, Akasaka T, et al. Quantitation of mitral valve tenting in ischemic mitral regurgitation by transthoracic real-time three-dimensional echocardiography. *J Am Coll Cardiol.* 2005;45:763-9.
16. McGee EC, Gillinov AM, Blackstone EH, Rajeswaran J, Cohen G, Najam F, et al. Recurrent mitral regurgitation after annuloplasty for functional ischemic mitral regurgitation. *J Thorac Cardiovasc Surg.* 2004;128:916-24.
17. Gillinov AM, Cosgrove DM 3rd, Shiota T, Qin J, Tsujino H, Stewart WJ, et al. Cosgrove-Edwards Annuloplasty System: midterm results. *Ann Thorac Surg.* 2000;69:717-21.
18. Flameng W, Herijgers P, Bogaerts K. Recurrence of mitral valve regurgitation after mitral valve repair in degenerative valve disease. *Circulation.* 2003;107:1609-1613.
19. Fasol R, Meinhart J, Deutsch M, Binder T. Mitral valve repair with the Colvin-Galloway Future Band. *Ann Thorac Surg.* 2004;77:1985-8.
20. Accola KD, Scott ML, Thompson PA, Palmer GJ 3rd, Sand ME, Ebra G. Midterm outcomes using the physio ring in mitral valve reconstruction: experience in 492 patients. *Ann Thorac Surg.* 2005;79:1276-83.
21. Fabricius AM, Walther T, Falk V, Mohr FW. Three-dimensional echocardiography for planning of mitral valve surgery: current applicability? *Ann Thorac Surg.* 2004;78:575-8.